SUPPRESSION OF CUTTING FORCES USING COMBINED INVERSE MODEL BASED DISTURBANCE OBSERVER AND DISTURBANCE FORCE OBSERVER

M. Maharof[1], Z. Jamaludin[1], M. Minhat[1], L. Abdullah[1], N. A. Anang[1], T. H. Chiew[2], J. Jamaludin[3] and T.Tjahjowidodo[4]

[1]Faculty of Manufacturing Engineering,
Universiti Teknikal Malaysia Melaka, Hang Tuah Jaya, 76100 Durian Tunggal, Melaka, Malaysia.

[2]Faculty of Engineering,
Tunku Abdul Rahman Universiti College,
Jalan Genting Klang, Setapak, 53300 Kuala Lumpur, Malaysia.

[3]Faculty of Engineering and Built Environment,
Jalan Menara Gading, UCSI Height, Cheras, 76000, Kuala Lumpur, Malaysia.

[4]School of Mechanical and Aerospace Engineering,
Division Mechatronics and Design, Nanyang Technological University, 50 Nanyang Avenue, Singapore 639798.

Corresponding Author's Email: [1]zamberi@utem.edu.my

Article History: Received 7 January 2018; Revised 16 June 2018; Accepted 22 September 2018

ABSTRACT: This paper focuses on damping strategies that addressed the effect that high frequency harmonics content of cutting force have on positioning accuracy of the x-axis of an XY positioning table via controller and observer design approaches. Cutting force generated from direct contact between the workpiece and cutting tool becomes input disturbance to the drive system of the positioning table. The force high frequency components if left undamped would generate vibration to the system thus affecting the system positioning accuracy, surface finish quality as well as tool life. For this purpose, a cascade P/PI position controller, an Inverse Model Based Disturbance Observer (IMBDO) and a Disturbance Force Observer (DFO) were designed and numerically analysed. The cascade P/PI controller was designed using traditional loop shaping frequency domain method. IMBDO estimates the input disturbance and any unmodelled system dynamics while DFO performs direct estimation of the cutting force using knowledge of harmonic frequencies corresponding to the input cutting force. A combined cascade P/PI controller with IMBDO and DFO reduced additional 3.83% and

1.90% tracking errors compared to separate application of IMBDO and DFO. This novel control approach produced between 34-80% greater reductions in peak amplitudes of the harmonics content of the cutting forces compared to cascade P/PI.

KEYWORDS: *Cascade Controller; Inverse Model Based Disturbance Observer (IMBDO); Disturbance Force Observer (DFO); Cutting Force; Disturbance Compensation*

1.0 INTRODUCTION

In control system, observers are used for number of purposes, such as removal of phase lag in feedback control loop, elimination for the needs of costly sensors [1] and estimation of input disturbance signals [2-3]. Observers complement position controllers in improving the control system ability to address issues relating to robustness against input disturbance that deteriorates control performance of a system. In case of milling cutting process, as the cutting force cannot be eliminated, a study by [4] has determined that inverse-model-based disturbance observer (IMBDO) is able to suppress for any kind of input disturbance. However, cutting force was compensated using state observer in [5] whereas techniques using IMBDO and repetitive controller were applied and their performances were compared for cutting force compensation in machine tool [6]. In all applications related to IMBDO, the accuracy of the system is a great concern as it affects the control bandwidth of the observer, as well as the performance and stability of the system. Besides IMBDO, a type of that belongs to a class of disturbance force observer (DFO) was presented in [7]. The technique involves estimation of the input disturbance signal using knowledge of the signal harmonic frequencies content. Experimental results in [7] showed the usefulness and effectiveness of DFO in force estimation and compensation for a system exposed to cutting force. In addition, [8] had implemented DFO to estimate input disturbance to improve tracking performance of a system. Also, DFO was applied by [9] in medical field for compensation of internal disturbance and external disturbance forces in medical tele-analyser. Results presented in [7-8] and [9] had demonstrated the effectiveness of DFO in suppressing impacts that input disturbance had on respective control performances. A variant of DFO named model-independent force observer was established

and presented in [10] as component of a haptic controller to measure force exerted by human hands. Works that have been presented showed the effectiveness of IMBDO and DFO as estimators and compensator for input disturbance signal. This paper extends the application of IMBDO and DFO by proposing a combined observer approach utilizing the strength of each observer. DFO explicitly estimates the cutting force while IMBDO estimates remaining discrepancies related to unmodelled system dynamics. This paper presents design analyses and control performances of a cascade P/PI position controller combined with (i) IMBDO, (ii) DFO and (iii) IMBDO plus DFO.

This paper is organized as follows. Experimental setup and system identification is introduced in Section 2. Milling cutting force characterization and analysis are described in Section 3 while the details design of cascade P/PI position controller and the disturbance observers, namely; IMBDO and DFO are explained in Section 4. Section 5 elaborates the numerical results and discussion and finally Section 6 concludes the findings with statements on future recommendation.

2.0 SYSTEM IDENTIFICATION

The system transfer function for the x-axis of the XY positioning table was identified according to [11]. For a single-input single-output (SISO) system, the frequency response function (FRF) of the system was estimated using H1 estimator [12] based on measured input voltage, $u(t)$ and output position signals, $z(t)$. A second order transfer function with time delay, T_d was fitted against the FRF using Fdident toolbox in MATLAB. Equation (1) shows the transfer function with gain $A = 78020 mm/Vs^2$; damper, $B = 163 s^{-1}$; stiffness, $C = 193.3 s^{-2}$ and $T_d = 0.0012 s$

$$G(s) = \frac{Z(s)}{U(s)} = \frac{A}{s^2 + Bs + C} e^{-sT_d} \quad (1)$$

Figure 1 shows diagram of the experimental setup that consists of (i) a personal computer fixed with MATLAB/Simulink software, (ii) a Digital Signal Processing unit (dSPACE DS1104), (iii) a Drives amplifier unit and (iv) an XY ballscrew driven positioning table. The host computer acts as a medium processing unit providing input in the form of reference tracking, monitoring of position measurements, and extracting control command input signal for corrective actions in relation to position tracking errors that were observed.

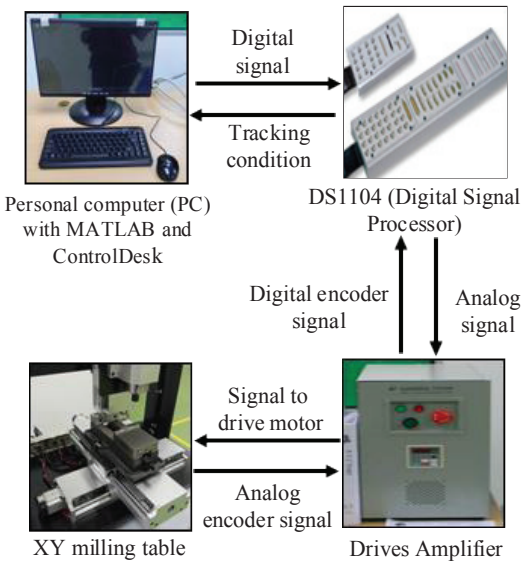

Figure 1: Schematic diagram of the experimental setup

3.0 CUTTING FORCE IDENTIFICATION

For numerical analysis purposes, actual cutting forces based on milling cutting process were captured and measured using Kistler Dynamometer measurement unit [13]. A straight-line cut was performed in the direction of x-axis as shown in Figure 2(a) using an aluminum block with HSS cutting tool of diameter 10mm at spindle speed rotation of 1500rpm. The measured cutting force characteristics was analysed in frequency domain method to identify the harmonic frequencies associated with 1500rpm of spindle speed rotation. Figure 2(b) shows Fast Fourier Transform (FFT) analysis of the measured cutting forces. The harmonic frequencies were identified at 26Hz, 52Hz and 78Hz.

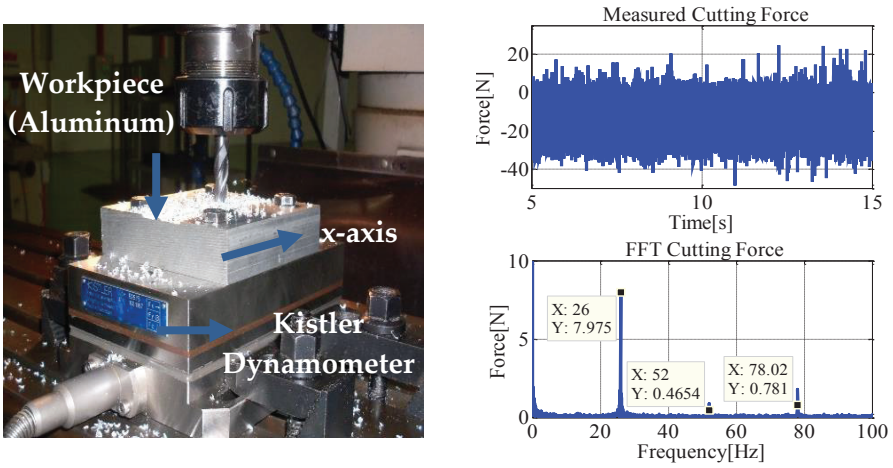

(a) (b)

Figure 2: (a) Measurement of milling cutting forces and (b) results of FFT analysis for x-axis

4.0 CONTROLLER AND OBSERVER DESIGN

4.1 Design of Cascade P/PI

A cascade P/PI controller [7] was designed for position control of the test setup. The controller consists of a Proportional Integral (PI) speed controller and a Proportional (P) position controller. Figure 3 shows schematic diagram of the control structure.

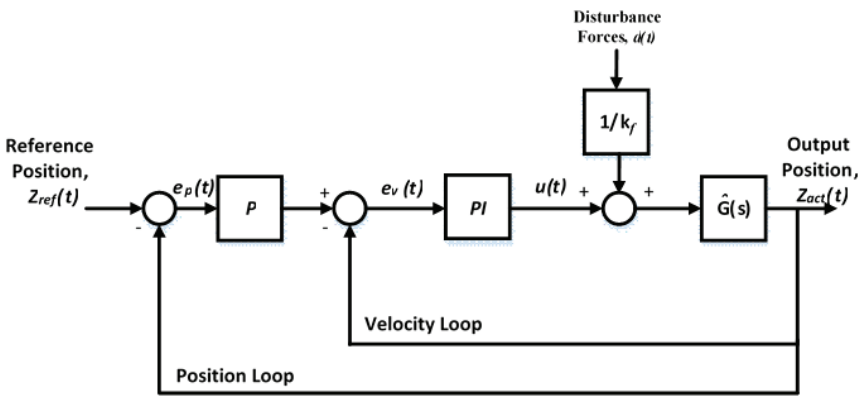

Figure 3: Schematic diagram of cascade P/PI controller

According to Figure 3, $Z_{ref}(t)$ and $Z_{act}(t)$ refer to input reference signal and output position signal measured in [mm] while $\hat{G}(s)$ is the system model transfer function. k_f is the motor constant in [N]/[V]. The controller gains were designed using frequency domain method based on gain and phase margin of the open loop transfer functions. The identified controller parameters are; $k_p = 0.00661$Vs/mm, $k_i = 0.12075$Vs^2/mm and $k_v = 225$s^{-1}. The overall bandwidth of the system identified based on the closed loop transfer function was 39.9Hz.

4.2 Design of IMBDO

The performance of cascade P/PI controller was enhanced by embedding IMBDO into the velocity loop of the control structure as shown in Figure 4. This resulted in overall bandwidth of the system at 41.6Hz. IMBDO was designed in such a condition that it produces only minimum effect to the open and closed loop characteristics of previously designed cascade P/PI controller. IMBDO did not alter the velocity and position loop characteristics of cascade P/PI controller to maintain desired control performance identified earlier.

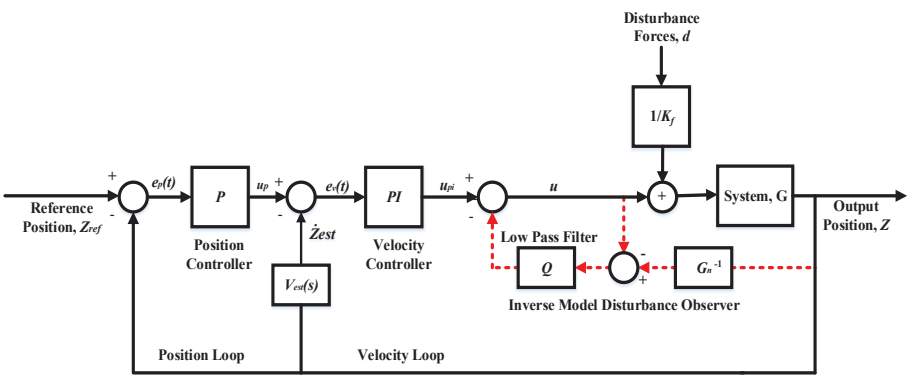

Figure 4: Schematic diagram of cascade P/PI with IMBDO

IMBDO consists primarily of a nominal plant transfer function, $G_n(s)$ and a low pass filter, Q(s) that was necessary to preserve stability [14]. The following equations are the transfer functions for $G_n(s)$ and Q(s) [14], respectively.

$$G_n(s) = 0 \tag{2}$$

$$Q(s) = \frac{\sum_{i=0}^{m} q_i s^i}{(s + \omega_c)^n} \tag{3}$$

where q_i's are the filter numerator coefficients, ω_c is the cut-off frequency while m and n are the orders of the numerator and denominator respectively, with n > m. In order to preserve stability, the *Q*-filter transfer function has to lie below the $|1/\Delta|$ line which was constructed based on Equation (4).

$$\Delta(f) = \frac{G(f) - G_n(f)}{G_n(f)} \tag{4}$$

Figure 5 compares the *Q*-filter transfer function and the $|1/\Delta|$ curve designed for $\omega_c = 90\text{Hz}$. The *Q*-filter cut-off frequency was selected as a trade-off between performance and stability. Increase in the frequency bandwidth of the *Q*-filter reduces the stability margins as the *Q*-filter line intersects the $|1/\Delta|$ curve resulting in instability.

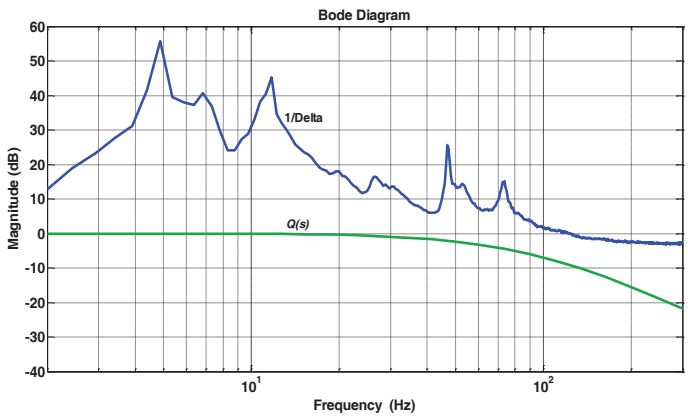

Figure 5: Bandwidth limitation of the *Q*-filter

4.3 Design of DFO

In the second control configuration, DFO was embedded into the cascade P/PI control configuration as shown in Figure 6.

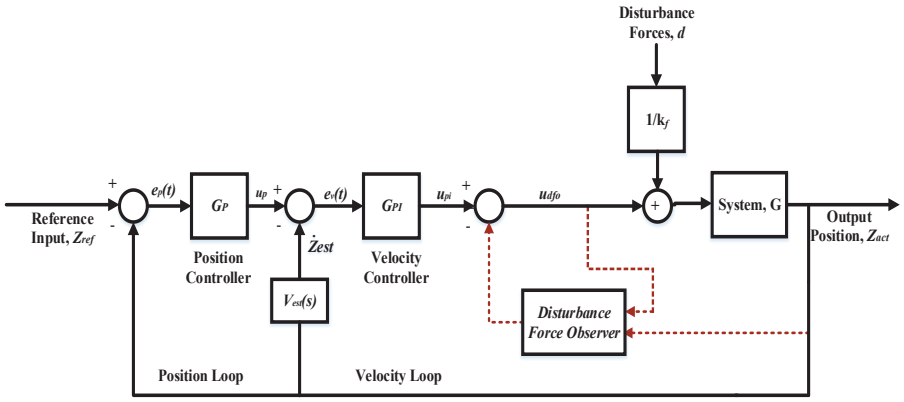

Figure 6: Schematic diagram of a cascade P/PI controller with DFO

DFO was established to estimate sinusoidal-based input disturbance signal. For this, consider a sinusoidal-based input disturbance force $d(t)$, the first derivative $\dot{d}(t)$, and second derivative $\ddot{d}(t)$:

$$d(t) = A'\sin(\omega t + \theta) \tag{5}$$

$$\dot{d}(t) = A'\,\omega\cos(\omega t + \theta) \tag{6}$$

$$\ddot{d}(t) = A'\,\omega^2\sin(\omega t + \theta) \tag{7}$$

where A is the signal amplitude, ω is the signal frequency, and θ is the offset value. A disturbance force observer was designed according to Equations (5)-(7). Equations (8) and (9) are the state space representation of the general order state space observer:

$$\dot{\hat{x}} = Fx + Gu + L(y - \hat{y}) \tag{8}$$

$$y = Hx \tag{9}$$

where x is the state variable matrix, y is the output, L and is the observer gain matrix. Equation (8) is the state space representation of

the system transfer function shown in Equation (1). Figure 7 shows schematic diagram of DFO based on Equation (10)-(11).

$$\begin{bmatrix} \dot{\hat{x}} \\ \dot{\hat{v}} \\ \dot{\hat{q}}_1 \\ \dot{\hat{q}}_2 \end{bmatrix} = \begin{bmatrix} 0 & 1 & 0 & 0 \\ 0 & -B & A & 0 \\ 0 & 0 & 0 & 1 \\ 0 & 0 & -\omega_2 & 0 \end{bmatrix} \begin{bmatrix} \hat{x} \\ \hat{v} \\ \hat{q}_1 \\ \hat{q}_2 \end{bmatrix} + \begin{bmatrix} 0 \\ A \\ 0 \\ 0 \end{bmatrix} \begin{bmatrix} u \end{bmatrix} + \begin{bmatrix} l_1 \\ l_2 \\ l_3 \\ l_4 \end{bmatrix} \left(y - \hat{y} \right) \tag{10}$$

$$y = \begin{bmatrix} 1 & 0 & 0 & 0 \end{bmatrix} \begin{bmatrix} \hat{x} \\ \hat{v} \\ \hat{q}_1 \\ \hat{q}_2 \end{bmatrix} \tag{11}$$

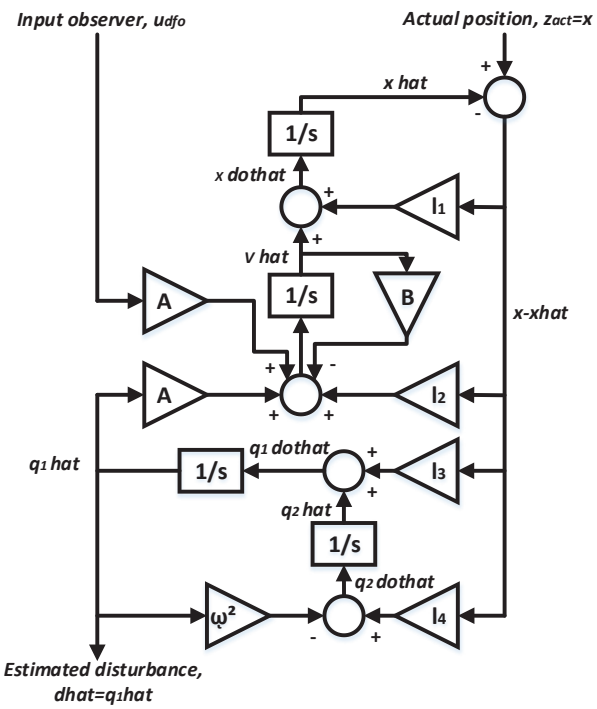

Figure 7: Schematic diagram of a DFO

4.4 Design of Combined IMBDO and DFO

The third control configuration consists of a cascade P/PI controller embedded with both IMBDO and DFO. The control structure is shown

in Figure 8. This is a novel control approach that combines the strength of both IMBDO and DFO to address issue relating to compensation of cutting forces in milling machine. Both IMBDO and DFO maintained their respective gain parameters as previously designed.

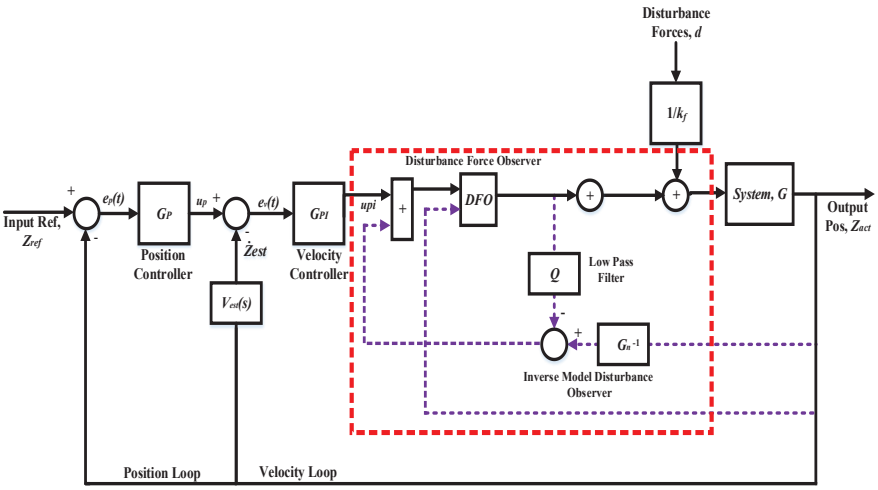

Figure 8: Schematic diagram of cascade P/PI controller embedded with IMBDO and DFO

5.0 RESULTS AND DISCUSSION

Numerical analyses were performed using the identified system transfer function and four control configurations were observed, namely; (i) cascade P/PI, (ii) cascade P/PI with IMBDO, (iii) cascade P/PI with DFO, and (iv) cascade P/PI with IMBDO plus DFO. The system was excited using input sinusoidal reference signal of amplitude 10mm at frequency of 0.5Hz and exposed to input disturbance in the form of measured cutting forces. The respective tracking errors were recorded and analysed in both time domain and frequency domain. Control performance analyses were performed based on; (i) Root Mean Square of Error (RMSE), (ii) Maximum Tracking Error (MTE) and (iii) Fast Fourier Transform (FFT) of the tracking errors. FFT analysis focuses on reduction in peak magnitudes of the force harmonic components that were identified earlier at 26Hz, 58Hz and 78Hz. Table 1 summarizes numerical results relating to RMSE and MTE values for the tracking errors obtained.

In general, the application of IMBDO and DFO have helped improved the control performance of stand-alone cascade P/PI controller. On average, IMBDO and DFO contributes 3.74% and 5.82 % further reduction in RMSE and MTE values compared to the benchmarked cascade P/PI controller. The lowest produced values of RMSE and MTE confirmed the added advantage of the combined control effort of both IMDBO and DFO. The RMSE values were further reduced by as much as 3.83% and 1.90% when compared to separate application of IMBDO and DFO respectively. Also, in term of MTE, the combined approach produced a further 5.10% and 1.63% reduction in MTE values compared to separate application of IMBDO and DFO.

Table 1: Numerical results of RMSE and MTE values for tracking errors

Control Configuration	RMSE [mm]	MTE [mm]
Cascade P/PI	0.1016	0.1477
Cascade P/PI with IMBDO	0.1017	0.1465
Cascade P/PI with DFO	0.0997	0.1414
Cascade P/PI with IMBDO plus DFO	0.0978	0.1391

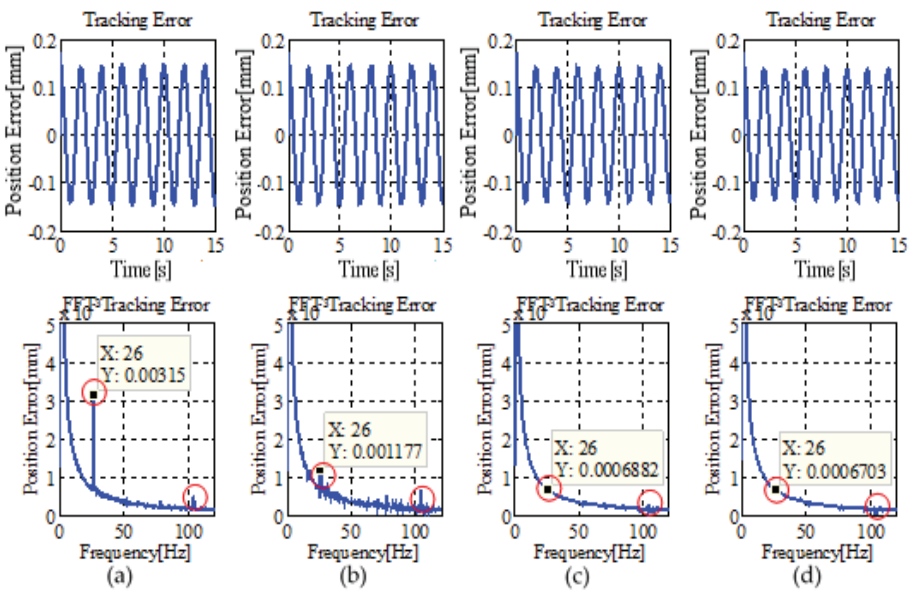

Figure 9: Numerical results of FFT on position errors for (a) cascade P/PI, (b) cascade P/PI with IMBDO, (c) cascade P/PI with DFO and (d) cascade P/PI of combined IMBDO and DFO

In frequency domain analysis, the control performance was analysed in term of reduction in peak amplitude values associated with the harmonic frequencies. Figure 9 shows results of FFT analysis performed on position tracking errors recorded by the respective controllers. Table 2 summarizes the peak amplitudes at the harmonic frequencies with corresponding values of the percentage error reduction obtained using cascade P/PI as the benchmarked control configuration. Results showed that maximum reduction in peak values at the multiple harmonic frequencies was observed in the case of cascade P/PI combined with IMBDO and DFO. This is expected since the control configuration utilizes both strengths of IMBDO and DFO to compensation unmodelled dynamics and errors associated with high frequencies component of the cutting force. Significant reduction was obtained at lower harmonics frequencies compared to harmonics at higher frequencies. This can be explained in term of the system bandwidth. The controllers were only able to compensate effectively for the range of frequencies that fall within the bandwidth of the system.

Table 2: Results of FFT analyses for different variants of cascade P/PI controller

Frequency [Hz]	Numerical Analysis Results FFT of Tracking Error [μm]			
	Cascade P/PI	IMBDO (%)	DFO (%)	Combined IMBDO and DFO (%)
26.00	3.1580	1.1770 (-62.7)	0.6882 (-78.2)	0.6703 (-78.8)
52.00	0.4511	0.3368 (-25.3)	0.3158 (-30.0)	0.2941 (-34.8)
78.00	0.3711	0.2681 (-27.8)	0.2453 (-33.9)	0.2412 (-35.0)

6.0 CONCLUSION

IMBDO and DFO produced the best tracking performance as reflected in lowest values of RMSE and MTE and highest reduction in peak amplitudes at the harmonics frequencies of the FFT results. The control configuration utilizes both strengths of IMBDO and DFO to compensate unmodelled dynamics and errors associated with high frequencies component of the cutting force. As for future work, the control performance could be further enhanced in terms of robustness against system uncertainties and process variations.

ACKNOWLEDGMENTS

The authors would like to thank the Ministry of Higher Education for the funding of this research with reference number FRGS/1/2015/TK03/FKP/02/F00281. The authors would also like to thank Faculty of Manufacturing Engineering, Universiti Teknikal Malaysia Melaka (UTeM) for the facilities provided.

REFERENCES

[1] G. Ellis, *Observers in Control Systems: A Practical Guide*. USA: Academic Press, 2002.

[2] T. Umeno and Y. Hori, "Robust speed control of DC servomotors using modern two degrees-of freedom controller design," *IEEE Transactions on Industrial Electronics*, vol. 38, no. 5, pp. 363–368, 1991.

[3] Y. Hori and K. Shimura, "Position/force Control of multi-axis robot manipulator based on the TDOF robust servo controller for each joint," in Proceedings of the American Control Conference, Chicago, Illinois, 1992, pp. 753–757.

[4] K. Ohnishi and T. Murakami, "Advanced motion control in robotics," in 15th Annual Conference of IEEE Industrial Electronics Society, Philadelphia, USA, 1989, pp. 356-359.

[5] S. Huang, K. Tan, G. S. Hong, and Y. S. Wong, "Cutting force control of milling machine," *Mechatronics*, vol. 17, no. 10, pp. 533-541, 2007.

[6] Z. Jamaludin, H. V. Brussel, G. Pipeleers, and J. Swevers, "Accurate motion control of XY high-speed linear drives using friction model feedforward and cutting forces estimation", *CIRP Annals-Manufacturing Technology*, vol. 57, no. 1, pp. 403-406, 2009.

[7] Z. Jamaludin, J. Jamaludin, T. H. Chiew, L. Abdullah, N. A. Rafan, and M. Maharof, "Sustainable cutting process for milling operation using disturbance observer", *Procedia CIRP*, vol. 40, pp. 486-491, 2016.

[8] J. G. Njiri, B.W. Ikua, and G. N. Nyakoe, "Cutting force control for ball end milling of sculptured surfaces using fuzzy logic controller", *Journal of Scientific Conference Proceedings*, pp. 249-255, 2012.

[9] A. Suebsomran and M. Parnichakun, "Disturbance observer-based hybrid control of displacement and force in medical tele-analyzer for abdominal mass analysis," in Industrial Technology, IEEE International Conference, Bangkok, Thailand, 2002, pp. 365-369.

[10] F. Mobasser and K. Hashtrudi-Zaad, "A model-independent force observer for teleoperation systems," in Mechatronics and Automation, IEEE International Conference, Niagara Falls, Canada, 2005, pp. 964-969.

[11] L. Abdullah, Z. Jamaludin, T. H. Chiew, N. A. Rafan, and M. S. Syed Mohamed. "System identification of XY table ballscrew drive using parametric and non-parametric frequency domain estimation via deterministic approach," *Procedia Engineering*, vol. 41, pp. 567-574, 2012.

[12] R. Pintelon and J. Schoukens, *System Identification: A Frequency Domain Approach*. New Jersey: John Wiley & Sons, 2012.

[13] M. H. Abu Bakar, R. A. Raja Izamshah and M. M. A. Amran,"Machining model of TI-6AL-4V titanium alloy using FEM simulation", *Journal of Advanced Manufacturing Technology*, vol. 6, no. 2, pp. 1-9, 2012.

[14] C. J. Kempf and S. Kobayashi, "Disturbance observer and feedforward design for a high-speed direct drive positioning table", *IEEE Transactions on Control System Technology*, vol. 7, no. 5, pp. 513-526, 1999.